DOI: 10.1002/chem.200800493

Fullerene Nanowires: Self-Assembled Structures of a Low-Molecular-Weight Organogelator Fabricated by the Langmuir–Blodgett Method

Ryo Tsunashima,[a] Shin-ichiro Noro,[a] Tomoyuki Akutagawa,[a, b] Takayoshi Nakamura,*[a, b] Hiroko Kawakami,[c] and Kazunori Toma[c]

Abstract: Fullerene derivative C60TT, which is substituted with the low-molecular-weight organogelator tris(dodecyloxy)benzamide, formed nanowire structures on application of the Langmuir–Blodgett (LB) method. The surface morphology of the C60TT LB film was dependent on the holding time before deposition at a surface pressure of 5 mN m^{-1}; it changed from a homogeneous monolayer to a bilayer fibrous structure via a fibrous monolayer structure, which was estimated to have dimensions of 1.2 nm in height, 8 nm in width, and 5–10 μm in length. From the structural and spectroscopic data, it is inferred that close packing of the fullerene moiety occurs along with intermolecular hydrogen bonding within the monolayer fibrous structure. The morphological changes in the LB film are explained kinetically by the Avrami theory, based on the decrease in the surface area of the monolayer at the air/water interface. The growth of the quasi-one-dimensional fibrous monolayer structures at holding times from 0 to 0.2 h is considered to be an interface-controlled process, whereas the growth of the quasi-one-dimensional bilayer fibrous structures from 0.2 to 18 h is thought to be a diffusion-controlled process.

Keywords: fullerenes · gels · nanostructures · self-assembly · thin films

Introduction

Since the discovery of [60]fullerene[1] and its macroscale synthesis,[2] researchers have identified a variety of exotic properties for the material, such as the existence of a superconducting transition at high temperature in alkali metal salts of [60]fullerene,[3,4] and a large third-order nonlinear optical response for thin films of [60]fullerene.[4] The remarkable physical characteristics of these materials has prompted the synthesis of a variety of fullerene derivatives for potential application as functional materials.[5–8] Chemical modification of fullerenes[5] has ranged from fullerene dyads[7] and a triad with porphyrin, showing photoinduced electron transfer with long-lived charge separation, to practical materials such as liquid crystals, in which a shuttlecock-shaped fullerene is stacked one-dimensionally in a head-to-tail manner to form a thermotropic hexagonal columnar phase.[8] While naked [60]fullerene exhibits isotropic intermolecular interaction as a result of its spherical shape, the liquid-crystal materials were constructed through self-assembly of modified fullerene derivatives that exhibit anisotropic intermolecular interactions and/or stacking of molecules.

These self-assembly processes are attracting considerable attention as a powerful tool for the construction of active nanoscale components, which will be required for future applications such as nanoscale electronic circuits. In particular, fiberlike assemblies will be important components in wiring and other active parts. Fullerenes are promising candidates for construction of such wiring materials, because they have a high charge mobility and exhibit metallic conducting behavior on carrier doping.[9,10] However, [60]fullerene tends to form two- or three-dimensional arrays in the aggregated state, and there have been only a few reports on the fabrication of fullerene-based, quasi-one-dimensional, fiberlike nanostructures.[11] To realize these nanostructures through self-assembly processes, it is essential to employ an appro-

[a] Dr. R. Tsunashima, Dr. S.-i. Noro, Prof. Dr. T. Akutagawa, Prof. Dr. T. Nakamura
Research Institute for Electronic Science
Hokkaido University, Sapporo 060-0812 (Japan)
Fax: (+81) 11-706-4972
E-mail: tnaka@es.hokudai.ac.jp

[b] Prof. Dr. T. Akutagawa, Prof. Dr. T. Nakamura
CREST, Japan Science and Technology Agency (JST)
Kawaguchi 332-0012 (Japan)

[c] Dr. H. Kawakami, Dr. K. Toma
The Noguchi Institute
Tokyo 173-00030 (Japan)

Supporting information for this article is available on the WWW under http://dx.doi.org/10.1002/chem.200800493.

priate molecular design and fabrication technique. In the present study, organogelators were adopted, and the LB technique was applied to construct fullerene nanowires.

Self-assembled fibrous structures have been observed in low-molecular-weight organogelators. In gels, fibrous structures become entangled to form three-dimensional networks,[12] which are constructed by self-assembly of gelators through intermolecular interactions such as one-dimensional hydrogen bonding. Several fullerene-based organogels have been reported.[13] Cholesterol-appended [60]fullerene showed gelation properties in dichloromethane.[13b] Modification of [60]fullerene to obtain strong one-dimensional intermolecular interactions, as is observed for gelators, will enable us to construct a quasi-one-dimensional array of [60]fullerene.

An excellent technique for immobilization of self-assembled nanostructures on solid substrates is the LB method.[14] Although the LB method has been used to prepare two-dimensional molecularly thin films, quasi-one-dimensional nanostructures have often been observed in LB monolayers,[15–17] for example, when molecules exhibit strong anisotropic intermolecular interactions. We have reported the formation of nanowires based on an amphiphilic bis(tetrathiafulvalene)-substituted macrocycle on a mica substrate using the LB method. As a result of one-dimensional π–π stacking and intermolecular S···S interaction between the tetrathiafulvalene moieties, nanowire structures were formed in the LB films.[16] In our investigations on LB films of organogelators, we recently reported the fabrication of nanofiber structures of a derivative of 3,4,5-tris(dodecyloxy)benzamide (ADT) on a solid substrate.[17] The molecule has an amphiphilic property in addition to gelation ability, which allows application of the LB method. In the LB films, fibrous structures with a height of 1.2 nm and a width of 50–100 nm were observed. The LB methods provided molecularly thin films, and therefore quasi-one-dimensional nanostructures with molecular-scale thickness could be obtained on a solid substrate.

Here we report on the fabrication of nanowire structures of a newly synthesized fullerene-linked 3,4,5-tris(dodecyloxy)benzamide derivative (C60TT) by the LB method. The molecular structures of ADT and C60TT are shown here. The 3,4,5-tris(dodecyloxy)benzamide moiety is an excellent organogelator framework;[17,18] therefore, fullerene-based fibrous structures with molecular thickness were expected in the LB films. C60TT formed organogels with chloroform and adopted a stable monolayer structure at the air/water interface. Formation of nanowire structures was confirmed by atomic force microscopy (AFM). A molecular model of quasi-one-dimensional assembled structures was constructed from structural and spectroscopic data. The Avrami theory successfully explains the mechanism of nanowire formation at the air/water interface.

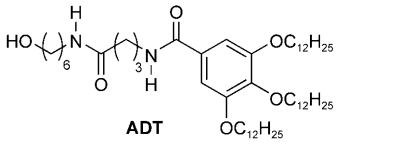

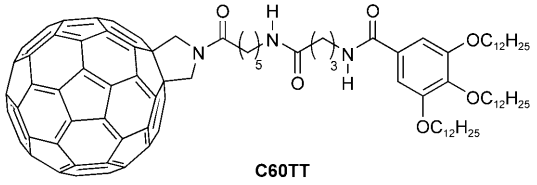

Results and Discussion

Synthesis and cast film of C60TT: C60TT was synthesized (Scheme 1, **1**–**7**) through amidation of fulleropyrrolidine[19] and *N*-{*N*-[3,4,5-tris(dodecyloxy)benzoyl]-4-aminobutyril}-6-aminohexanoic acid (**6**). Treatment of *N*-triphenylmethylpyrrolidine-C_{60} with trifluoromethanesulfonic acid in pyridine gave fulleropyrrolidine (**7**), which was directly treated with **6**. C60TT thus obtained was purified by HPLC (chloroform). The C60TT is insoluble in common solvents such as aliphatic alcohols, acetone, and hexane. An organogel was formed by a chloroform solution of C60TT at 277 K.[20] However, the cast film of C60TT did not exhibit a xerogel-like structure. A layered grain structure, each layer of which has a height of 6.0 nm, was observed in the AFM image of the cast film fabricated from chloroform solution at room temperature (see Supporting Information). From the XRD measurement, a face spacing of 5.96 nm was confirmed (see Supporting Information). Taking the length of the molecule into account, the molecules formed multilayer structures in each of the grain structures. Similar disklike structures have been reported in a fullerene amphiphile in a film cast from aqueous solution with a height 4–5 times larger than the length of the molecule.[21]

Langmuir–Blodgett film of C60TT: Figure 1 shows the surface pressure–area (π–A) isotherm of C60TT. The surface pressure began to increase at around $A = 1.45\ nm^2$. On further compression, the surface pressure decreased at $8.6\ mN\,m^{-1}$, which suggests either collapse of the Langmuir film or a phase transition. Langmuir films of C60TT were transferred onto mica substrates by single withdrawal after waiting for 0, 0.2, 1.5 or 18 h at a surface pressure of $5\ mN\,m^{-1}$.

The AFM images of the LB films are shown in Figure 2. The surface morphology is dependent on the holding time at $5\ mN\,m^{-1}$ before deposition. The transfer ratio of each film was almost unity in all cases. At 0 h, a homogeneous monolayer with a thickness of 0.9 nm occupied the major part of the surface. Fibrous structures with a height of 1.2 nm and a width of 13 nm were also observed. Taking convolution effects into account (see Supporting Information),[22] the actual width of the fibrous structures is 8 nm. The surface coverage of the fibrous structure increased with increasing holding time and became dominant at 0.2 h. These fibrous

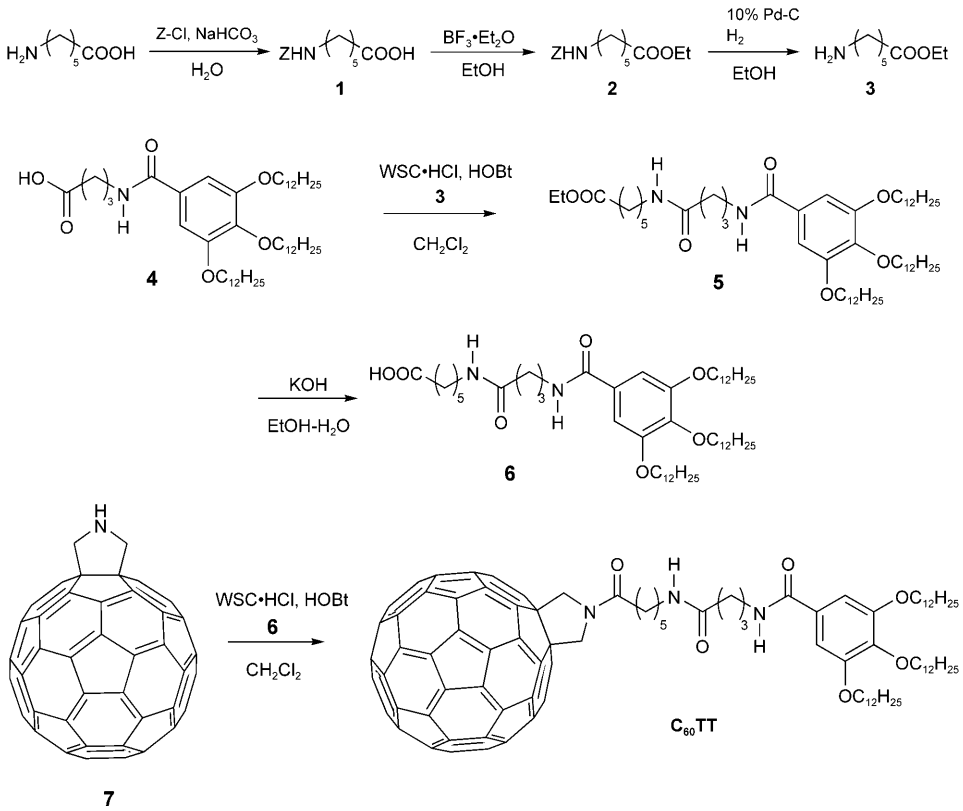

Scheme 1. Synthesis of C60TT. Z = benzyloxycarbonyl, WSC = water-soluble carbodiimide, HOBt = hydroxybenzotriazole.

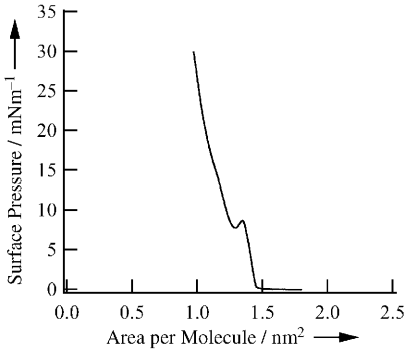

Figure 1. π–A isotherm of C60TT.

structures are considered to be of monolayer thickness, based on the diameter of the fullerene. As such, we refer to the fibrous structures as monolayer fibrous structures hereafter.

In the AFM image of the film deposited after 1.5 h, a fibrous structure with a height of 1.7 nm was observed. The height was almost twice that of the homogeneous monolayer; this suggests a bilayer structure. The coverage of the bilayer fibrous structure increased with increased holding time. From AFM observations, a transition between two morphologies could be observed with increasing holding time at the air/water interface. The first morphology was a monolayer fibrous structure, and the second a bilayer fibrous structure. The fact that the morphology of the films deposited on the solid substrate did not change after standing for one day suggests that the morphological changes occurred at the air/water interface as a result of holding the Langmuir films at 5 mN m^{-1}.

The surface coverage of the homogeneous monolayer (x^{L}_{homo}) and the monolayer fibrous structure (x^{L}_{fib}) at the air/water interface was estimated from the surface area of the Langmuir film and the height of each structure (see Supporting Information). The values were then compared with those on a mica substrate (x^{LB}_{homo} and x^{LB}_{fib} for homogeneous monolayer and monolayer fibrous structure, respectively), as estimated from the AFM images after 0.2 h. The results are summarized in Table 1. The surface coverage x^{LB}_{fib} was estimated to be 0.4, which is much smaller

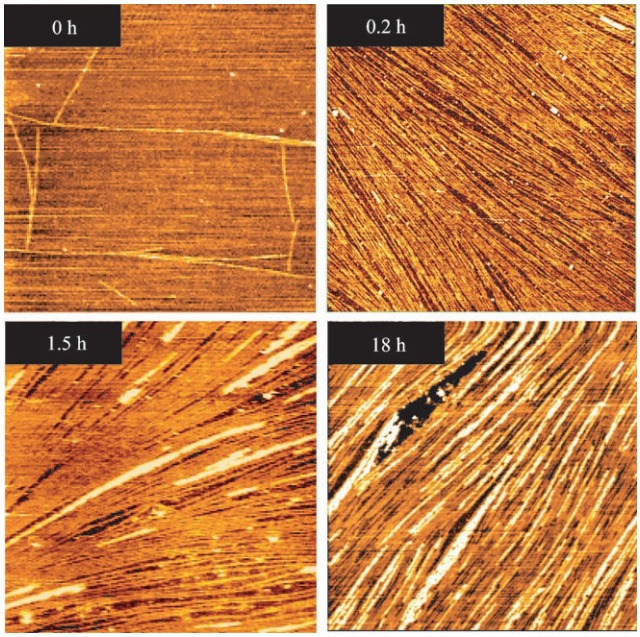

Figure 2. AFM images (2×2 μm) of LB films on a mica substrate formed by a single withdrawal after 0, 0.2, 1.5, and 18 h waiting time at 5 mN m^{-1}.

than that expected from the corresponding AFM image in Figure 2 when the convolution effect is taken into account

Table 1. Surface area (SA) and surface coverage x of the homogeneous monolayer (homo) and monolayer fibrous structure (fib) estimated from AFM images (LB) and the surface area at the air/water interface (L) at 0.2 h.

Holding time [h]	SA [nm^2]	x^{L}_{homo}	x^{LB}_{homo}	x^{L}_{fib}	x^{LB}_{fib}
0.2	1.29	0.7	0.6	0.3	0.4

(see Supporting Information). The x^{LB}_{fib} and x^{L}_{fib} values showed good correspondence, that is, the structures of the Langmuir film at the air/water interface and the LB film on the solid substrate are similar. In addition, the area per molecule in the monolayer fibrous structure at the air/water interface was calculated to be 1.0 nm^2, which corresponds to the cross-sectional area of naked [60]fullerene[23] and suggests close packing of fullerene moieties in the monolayer fibrous structures.

FTIR and UV/Vis spectroscopy of C60TT and ADT: IR spectroscopy is a powerful technique for the characterization of intermolecular interactions.[24] A large number of studies of intermolecular interactions in molecular assemblies, such as thin films, gels, and liquid crystals, have been reported.[24b,d–i] Intermolecular interactions in the assembled structures of C60TT were investigated by IR spectroscopy. C60TT can form a gel at lower temperatures, so it was difficult to investigate details of physical and structural properties of the gel by IR spectroscopy. However, as C60TT is composed of ADT and [60]fullerene, the structural details of ADT were characterized and compared with those of LB films of C60TT. ADT forms stable orgnanogels at room temperature with, for example, CCl_4.[17]

Figure 3a shows IR spectra for solutions of ADT in CCl_4 (1–10 mM) and the ADT gel. Once the 10 mM solution was cooled to 277 K, gelation occurred and the gel was stable at room temperature. The band observed at 2855 cm^{-1} (see Supporting Information) was assigned to the C–H stretching mode of ADT.[24i] All spectra taken in CCl_4 were normalized

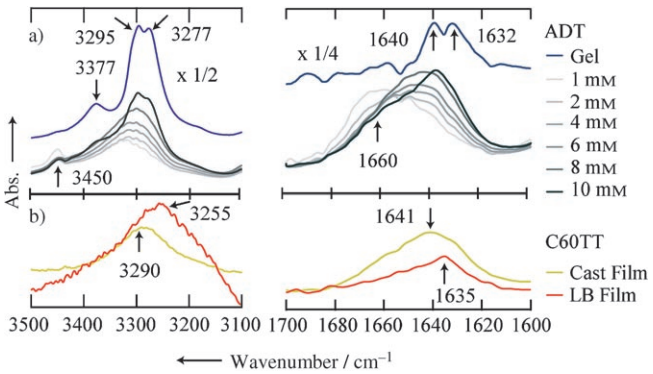

Figure 3. FTIR spectra in the ranges 3100–3500 cm^{-1} and 1600–1700 cm^{-1} of a) ADT in CCl_4 solution (1, 2, 4, 6, 8, 10 mM) and CCl_4 gel (10 mM) and b) cast and 40-layer LB films of C60TT. The CCl_4 gel spectra were reduced by one-half (3100–3500 cm^{-1}) and one-quarter (1600–1700 cm^{-1}) for ease of comparison.

relative to the C–H stretching band. In the region from 1600–1700 cm^{-1} for the 1 mM solution, the band observed at 1660 cm^{-1} was assigned as a free C=O vibrational band based on previous reports.[24b–i] This free C=O band decreased with increasing concentration. At the same time, a new band at 1640 cm^{-1} appeared and increased, and this was assigned as a hydrogen-bonding C=O band.[24b–i] In the region of 3100–3500 cm^{-1} in the 1 mM solution, two bands at 3322 and 3450 cm^{-1} were assigned to free and hydrogen-bonding N–H vibrational bands, respectively.[24c–i] With increasing concentration, the hydrogen-bonding N–H band showed a redshift to 3295 cm^{-1} with increased intensity. In addition, a new band appeared at 3377 cm^{-1} in the 10 mM solution, which was assigned to the hydrogen-bonding O–H vibrational mode.[24a,k] The series of intensity increases of the hydrogen-bonding C=O, N–H, and O–H bands with increasing concentration indicates an increase in the proportion of hydrogen-bonded species. The bands observed for the gel state were assigned to hydrogen-bonding C=O (1632 and 1640 cm^{-1}), N–H (3277 and 3295 cm^{-1}), and O–H (3377 cm^{-1}). Compared with those of the 10 mM solution, the bands for free C=O and N–H almost disappeared, and the hydrogen-bonding C=O and N–H bands split into two different bands. This indicates the existence of two different types of hydrogen-bonded C=O and N–H species in the gel. From the relationship between the N···O distance and the wavenumber of the C=O vibrational band,[24c] they were estimated as 2.891 (1640) and 2.865 Å (1632 cm^{-1}). These results indicate that the main driving force for gel formation is intermolecular hydrogen bonding between amide moieties and between terminal O–H groups.

Figure 3b shows IR spectra of the LB film deposited after holding for 0.2 h at 5 mN m^{-1} and the cast film of C60TT. The C=O and N–H bands of the LB film were observed at 1635 and 3255 cm^{-1}, respectively. In the cast film, these bands appeared at 1641 and 3290 cm^{-1}, respectively. Although these bands were assigned to hydrogen-bonding C=O and N–H bands, the bands in the LB films were observed at slightly lower wavenumbers than those in the cast film. This results from the difference in the N···O distances between adjacent molecules in each of the films. The relationship of the N···O distances and the wavenumbers of the C=O vibration bands[24c] suggests that stronger hydrogen bonds are formed in the LB film than in the cast film. Since the shape of the assembled structures is generally governed by intermolecular interactions, these differences in hydrogen bonding are responsible for the different surface morphologies of the LB and cast films. The C=O and N–H bands of the LB film of C60TT were observed at similar or lower wavenumber than those of the ADT gel, that is, C60TT in the LB film forms strong hydrogen bonds comparable to those in the ADT gel.

The fullerene moieties showed typical absorption bands due to overlap of adjacent π orbitals in the UV/Vis region.[4] In the UV/Vis region (see Supporting Information), a π–π* transition of the fullerene moiety was observed at 30×10^3 to 32×10^3 cm^{-1}, in addition to a broad shoulder around $22\times$

$10^3\ cm^{-1}$. The latter band is related to intermolecular interaction between adjacent fullerene moieties.[4]

Thus, the IR and UV/Vis spectra indicate the existence of intermolecular hydrogen-bonding and π–π interactions between the fullerene moieties. From the AFM images, the monolayer fibrous structures were estimated to be 1.2 nm high and 8 nm wide. Close packing of the fullerene moieties in the monolayer fibrous structures was also suggested by the π–A isotherm. From these results, we can infer a possible molecular model for the monolayer fibrous structures (Figure 4). Close packing of the fullerene moieties through

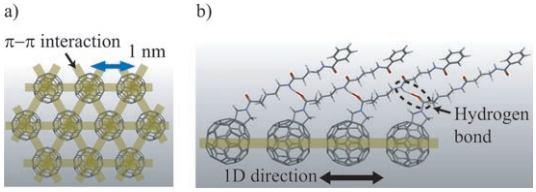

Figure 4. Schematic molecular model of the monolayer fibrous structure (C gray, N red, O blue).

π–π interactions is expected in the film plane (Figure 4a). The side chains should be aligned through intermolecular hydrogen bonding between amide groups of the alkyl amide moiety adjacent to the pyrrolidine moiety (Figure 4b). Taking the height (1.2 nm) of the monolayer fibrous structure into account, it is considered that the long axis of the molecule is tilted with respect to the axis normal to the substrate.

Formation mechanism of nanowires: To explain the origin of the structural changes at the air/water interface, the Avrami theory[25] was applied. The Avrami equation has been used to explain the crystal growth of polymers,[25c] gelation,[26] and structural changes in Langmuir films at the air/water interface.[27] The formation and growth mechanisms of the monolayer and bilayer fibrous structures at the air/water interface were considered in terms of the change in surface area over time. The change in area per molecule while holding at $5\ mN\,m^{-1}$ $A_5(t)$ was plotted against holding time (Figure 5). The $A_5(t)$ value decreased with time and became constant at $1.09\ nm^2$ [$A_5(\infty)$]. The normalized area A^* is defined by Equation (1), which corresponds to the fractional decrease in area at time t.

$$A^* = \{A(t)-A(\infty)\}/\{A(0)-A(\infty)\} \quad (1)$$

In the $\ln(\ln A^*)$ versus $\ln t$ plot (Figure 5), two different slopes were observed: 2.0 from 0 to 0.2 h, and 0.61 from 0.2 to 18 h. The AFM images of the transferred films also showed two types of surface morphology, with a transition at 0.2 h. Therefore, the transition observed in Figure 5 is likely related to structural changes in the Langmuir film at the air/water interface. The kinetics of the normalized area A^* are described by the Avrami equation [Eq. (2)], in which

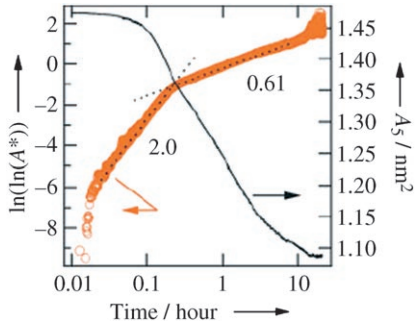

Figure 5. Time dependence of the area per molecule at a surface pressure of $5\ mN\,m^{-1}$ (A_5) for the C60TT Langmuir film (right axis). The red circles show the observed normalized area A^* (see text). The dotted lines show a linear fit of $\ln(\ln A^*)$ against $\ln t$ (left axis).

the Avrami index n is obtained from the slope of the $\ln(\ln A^*)$ versus $\ln t$ plot.

$$A^* = \exp(-kt^n) \quad (2)$$

The Avrami index n is generally expressed by Equation (3),in which the parameters h, k, and l relate to the processes of nucleation, crystal growth, and growth habit, respectively.[25–27]

$$n = h + kl \quad (3)$$

From t=0–0.2, n was estimated to be 2.0. Formation of quasi-one-dimensional fibrous structures was observed in the AFM image, and because the monolayer fibrous structures did not grow in the width direction, we assumed that l=1 and hence h=k=1. Thus, the monolayer fibrous structures are considered to form by homogeneous nucleation (h=1) and interface-controlled growth (k=1). Similar processes governed by one-dimensional growth have been reported in the formation of fibrous structures of gelators.[26] On holding the Langmuir film at $5\ mN\,m^{-1}$, molecules in the homogeneous monolayer assemble to create a monolayer fibrous structure at the growth interface.

After 0.2 h, bilayer fibrous structures were formed and grew. The index n is estimated to be 0.5, based on the slope of 0.61. The h, k, and l parameters are therefore assumed to be 0, 0.5, and 1, respectively. Thus, the quasi-one-dimensional bilayer fibrous structures (l=1) are thought to form by heterogeneous nucleation (h=0) and diffusion-controlled growth (k=0.5). After 0.2 h, homogeneous monolayer and monolayer fibrous structures were present at the air/water interface. If the bilayer fibrous structures are formed through assembly of molecules from the homogeneous monolayer, as occurs in the formation of monolayer fibrous structures, then the kinetics would be governed by an interfacial process. However, if the bilayer fibrous structures are formed by the assembly of monolayer fibrous structures, then nucleation and growth would occur as a result of close contact of the monolayer fibrous structures by a diffusion process. The mobility of fibrous structures at the air/water

interface should be low, and therefore the growth of bilayer fibrous structures should always be governed by diffusion. In fact, the growth rate of the bilayer structures was much slower than that of the monolayer fibrous structures. Similar diffusion-controlled growth was also reported for crystallization of a polymer in a melt with a large amount of noncrystallizable impurities.[28] Figure 6 shows a schematic view of

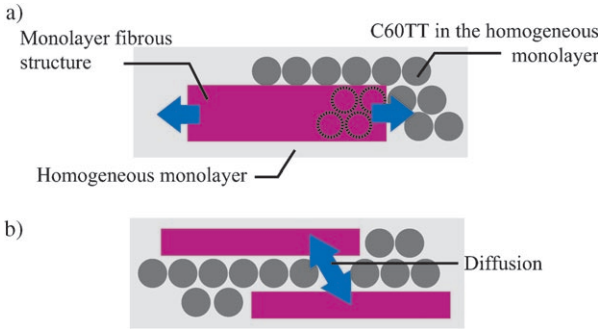

Figure 6. Mechanism for the formation of a) a monolayer fibrous structure and b) a bilayer fibrous structure.

the overall change in structure, from the homogeneous monolayer to the bilayer fibrous structure via the monolayer fibrous structures. The monolayer fibrous structures are formed by an interface-controlled process, and these structures then assemble to form bilayer fibrous structures by a diffusion-controlled process.

Conclusion

Fullerene nanowires were fabricated from a newly synthesized low-molecular-weight organogelator (C60TT). In contrast to the formation of grain structure in the cast film, monolayer fibrous structures of 1.2 nm in height, 5–10 μm in length, and 8 nm in width were obtained by the LB method. Infrared spectroscopy indicated that C60TT in the LB film is involved in hydrogen bonding comparable to that in the ADT gel. UV/Vis spectroscopy suggested π–π interactions between the fullerene moieties in the LB film. A molecular model of the monolayer fibrous structure was constructed on the basis of the structural and spectroscopic data. The surface morphology of the LB film depends on the holding time at the air/water interface before deposition. A change from a homogeneous monolayer structure to monolayer fibrous structures was observed over 0.2 h, and growth of bilayer fibrous structures after 0.2 h. The morphological changes were considered to originate from structural changes at the air/water interface, and were explained by Avrami theory. From 0 to 0.2 h, monolayer fibrous structures formed by homogeneous nucleation and quasi-one-dimensional interface-controlled growth from molecules in the homogeneous monolayer. After 0.2 h, bilayer fibrous structures formed by assembly of the monolayer fibrous structures through heterogeneous nucleation and quasi-one-dimensional diffusion-controlled growth. Use of low-molecular-weight organogelators and the LB method are proposed for the development of methods of fabrication of self-assembling nanowires. In addition, Avrami theory provided a kinetic mechanism for formation of the fibrous structures. [60]Fullerene and its derivatives have high carrier mobility and can be utilized in field-effect transistors.[29] These properties are also expected in the fullerene nanowires obtained in this study, and further research will seek to determine whether this is so.

Experimental Section

Film preparation: A conventional Langmuir trough (NIMA 5152D) was used for Langmuir film formation and LB film deposition. A chloroform solution of C60TT (0.5 mM) was spread on a pure water surface. The π–A isotherms were recorded at 291 K and a barrier speed of 100 mm min^{-1}. Films for AFM observations were deposited at a surface pressure of 5 mN m^{-1} by single up-stroke withdrawal of a mica substrate at 5 mm min^{-1} (vertical dipping method) after a certain holding time. The 40-layer LB films were transferred at 5 mN m^{-1} after holding for 0.2 h by a horizontal-lifting method onto solid substrates. Hydrophobized CaF_2 and quartz substrates were used for recording IR and UV/Vis spectra, respectively.

Atomic force microscopy: AFM images were taken under ambient conditions with a SPA-400 multifunction unit equipped with an SPI 3800 probe station (SII NanoTechnology Inc.) or a JEOL JSPM-5200 Environmental Scanning Microscope operating in dynamic force mode and/or contact mode by using commercially available silicon nitride cantilevers with a spring constant of 15 N m^{-1}.

Characterization: IR and UV/Vis spectra were measured on a Perkin–Elmer Lambda-19 spectrophotometer and a Perkin–Elmer Spectrum 2000 spectrometer, respectively.

Synthesis: C60TT was synthesized according to Scheme 1. ADT, compound **4**, and *N*-triphenylmethylpyrrolidine-C_{60} were prepared according to previously reported methods.[17,19] All reagents and solvents were purchased from commercial suppliers and were used as provided. Compounds were characterized by ^{1}H NMR spectroscopy, mass spectroscopy and elemental analysis.

***N*-Benzyloxycarbonyl-6-aminohexanoic acid (1)**: 6-Aminohexanoic acid (1.42 g, 13.8 mmol) and $NaHCO_3$ (1.73 g, 20.6 mmol) were dissolved in water (20 mL). Benzyloxycarbonyl chloride (2.4 mL, 16.8 mmol) was added dropwise to the mixture at 0 °C, which was stirred at room temperature for 18 h. The resulting precipitate was collected by filtration and washed with hexane. The aqueous layer was acidified with 1 N HCl and extracted with $CHCl_3$. The organic layer was washed with saturated aqueous NaCl, dried over Na_2SO_4, and concentrated in vacuo. The resulting residue and precipitate were combined and purified by silica-gel column chromatography (hexane/EtOAc 1:1) to afford **1** (2.34 g, 8.81 mmol, 95 %). ^{1}H NMR ($CDCl_3$, TMS): δ = 1.37 (quint, J = 7.6 Hz, 2H), 1.53 (quint, J = 7.6 Hz, 2H), 1.65 (quint, J = 7.6 Hz, 2H), 2.35 (t, J = 7.6 Hz, 2H), 3.20 (q, J = 7.6 Hz, 2H), 4.77 (m, 1H), 5.27 (s, 2H), 7.36 ppm (m, 5H).

Ethyl *N*-benzyloxycarbonyl-6-aminohexanoate (2): BF_3·Et_2O (0.5 mL, 2.37 mmol) was added to a solution of **1** (1.08 g, 4.04 mmol) in EtOH (20 mL) and the mixture was heated to reflux for 2 h. The reaction mixture was quenched with Et_3N (2 mL) and concentrated in vacuo. The residue was purified by column chromatography on silica gel (hexane/EtOAc 8:2) to give **2** (1.12 g, 3.83 mmol, 94 %). ^{1}H NMR ($CDCl_3$, TMS): δ = 1.25 (t, J = 6.9 Hz, 3H), 1.36 (quint, J = 7.6 Hz, 2H), 1.52 (quint, J = 7.6 Hz, 2H), 1.64 (quint, J = 7.6 Hz, 2H), 2.29 (t, J = 7.6 Hz, 2H), 3.20 (q, J = 7.6 Hz, 2H), 4.12 (q, J = 6.9 Hz, 2H), 4.74 (m, 1H), 5.09 (s, 2H), 7.36 ppm (m, 5H).

Ethyl 6-aminohexanoate (3): A solution of **2** (1.10 g, 3.76 mmol) in EtOH (20 mL) was stirred in the presence of 10% Pd/C (150 mg) at room temperature under an H_2 atmosphere. After stirring for 18 h, the Pd/C was removed by filtration through Celite to provide a solution of **3** in EtOH, which was directly used for the synthesis of **5**.

Ethyl *N*-{*N*-[3,4,5-tris(dodecyloxy)benzoyl]-4-aminobutyril}-6-aminohexanoate (5): Compound **4** (843 mg, 1.11 mmol), 1-hydroxybenzotriazole hydrate (203 mg, 1.33 mmol), and water-soluble carbodiimide·HCl (260 mg, 1.36 mmol) were dissolved in CH_2Cl_2 (30 mL). The mixture was stirred at room temperature for 1 h, and then the above-mentioned solution of **3** in EtOH was added to the solution. After stirring at room temperature for 2 h, the reaction mixture was diluted with CH_2Cl_2 and washed with saturated aqueous $NaHCO_3$. The organic layer was dried over Na_2SO_4 and concentrated in vacuo. The resulting residue was recrystallized from MeOH to yield **5** (956 mg, 1.06 mmol, 96% from **4**). ^{1}H NMR ($CDCl_3$, TMS): $\delta = 0.88$ (t, $J = 7.6$ Hz, 9H), 1.24–1.36 (m, 53H), 1.49 (m, 8H), 1.62 (quint, $J = 7.6$ Hz, 2H), 1.73 (quint, $J = 7.6$ Hz, 2H), 1.81 (quint, $J = 7.6$ Hz, 4H), 1.96 (m, 2H), 2.28 (t, $J = 7.6$ Hz, 2H), 2.32 (t, $J = 6.2$ Hz, 2H), 3.24 (q, $J = 6.2$ Hz, 2H), 3.49 (q, $J = 6.2$ Hz, 2H), 3.98 (t, $J = 6.9$ Hz, 2H), 4.03 (t, $J = 6.9$ Hz, 4H), 4.11 (q, $J = 6.9$ Hz, 2H), 6.03 (t, $J = 6.2$ Hz, 1H), 7.04 (s, 2H), 7.10 ppm (t, $J = 6.2$ Hz, 1H).

***N*-{*N*-[3,4,5-Tris(dodecyloxy)benzoyl]-4-aminobutyril}-6-aminohexanoic acid (6)**: A solution of KOH (421 mg, 7.50 mmol) in water (8 mL) was added to **5** (930 mg, 1.03 mmol) in EtOH (30 mL), and the mixture stirred at 40 °C for 30 min. The reaction mixture was neutralized with 1 N HCl and extracted with $CHCl_3$. The organic layer was washed with saturated aqueous NaCl, dried over Na_2SO_4, and concentrated in vacuo. The resulting residue was recrystallized from MeOH to give **6** (854 mg, 0.978 mmol, 95%). ^{1}H NMR ($CDCl_3$, TMS): $\delta = 0.88$ (t, $J = 7.6$ Hz, 9H), 1.24–1.34 (m, 50H), 1.46 (m, 8H), 1.63 (quint, $J = 7.6$ Hz, 2H), 1.73 (quint, $J = 6.8$ Hz, 2H), 1.81 (quint, $J = 7.6$ Hz, 4H), 1.97 (quint, $J = 6.9$ Hz, 2H), 2.30 (t, $J = 6.9$ Hz, 2H), 2.33 (t, $J = 6.9$ Hz, 2H), 3.26 (q, $J = 6.2$ Hz, 2H), 3.49 (q, $J = 6.2$ Hz, 2H), 3.99 (t, $J = 6.9$ Hz, 2H), 4.03 (t, $J = 6.9$ Hz, 4H), 6.03 (m, 1H), 6.87 (m, 1H), 7.02 ppm (s, 2H).

Fullerene-linked 3,4,5-tris(dodecyloxy)benzamide derivative C60TT: A solution of **6** (55 mg, 0.063 mmol), water-soluble carbodiimide·HCl (14 mg, 0.073 mmol), and 1-hydroxybenzotriazole hydrate (9 mg, 0.058 mmol) in CH_2Cl_2 (7 mL) was stirred in an ice bath for 1 h under an Ar atmosphere (solution I). CF_3SO_3H (0.1 mL) was added to a suspension of *N*-triphenylmethylpyrrolidine-C_{60} (42 mg, 0.041 mmol) in CH_2Cl_2, and the mixture stirred for 1 h. The resulting precipitate was collected by centrifugation, washed several times with wet diethyl ether, and then dried. The obtained solid was suspended in CH_2Cl_2 (5 mL) together with 4-dimethylaminopyridine (4 mg) and pyridine (0.5 mL) and added to solution I. After 3 h of stirring under an Ar atmosphere, the brownish solution was diluted with CH_2Cl_2. The organic layer was washed with dilute HCl, water, and saturated aqueous NaCl, and then dried over $MgSO_4$ and concentrated in vacuo. After purification by HPLC (chloroform), C60TT was obtained (10 mg, 0.0062 mmol, 10% from **6**). ^{1}H NMR ($CDCl_3$, TMS): $\delta = 0.88$ (t, $J = 6.8$ Hz, 9H), 1.2–1.3 (m, 48H), 1.46 (m, 4H), 1.57 (m, 2H), 1.63 (m, 2H), 1.73 (m, 4H), 1.81 (m, 6H), 1.95 (m, 4H), 2.36 (t, $J = 5.7$ Hz, 2H), 2.80 (t, $J = 7.3$ Hz, 2H), 3.35 (q, $J = 6.2$ Hz, 2H), 3.50 (q, $J = 6.2$ Hz, 2H), 3.97 (t, $J = 6.2$ Hz, 2H), 4.03 (t, $J = 6.6$ Hz, 2H), 5.36 (s, 2H), 5.45 (s, 2H), 6.29 (t, $J = 5.7$ Hz, 1H), 7.06 (s, 2H), 7.17 ppm (t, $J = 5.3$ Hz, 1H); elemental analysis (%) calcd for $C_{115}H_{99}N_3O_6$: C 85.31, H 6.16, N 2.60; found: C 83.51, H 6.06, N 2.58; FABMS: *m*/*z*: calcd for $[M+H]^+$: 1619; found: 1618.8.

Acknowledgement

This work was partly supported by a Grant-in-Aid for Science Research from the Ministry of Education, Science, Sports and Culture of Japan.

[1] H. W. Kroto, J. R. Heath, S. C. O'Brien, R. F. Curl, R. E. Smalley, *Nature* **1985**, *318*, 162.

[2] W. Krautschmer, L. D. Lamb, K. Fostirpoulos, D. R. Huffman, *Nature* **1990**, *347*, 354.

[3] a) R. C. Haddon, A. F. Hebard, M. J. Rosseinski, D. W. Murphy, S. J. Duclos, K. B. Lyons, B. Miller, J. M. Zahurak, R. Tycko, G. Dabbagh, F. A. Thiel, *Nature* **1991**, *350*, 320; b) K. Holczer, O. Klein, S.-M. Huang, R. B. Kaner, K.-J. Fu, R. L. Whetten, F. Diederich, *Science* **1991**, *252*, 1154.

[4] a) L. W. Tutt, A. Krost, *Nature* **1992**, *356*, 225; b) *Optical and Electronic Properties of Fullerenes and Fullerene-Based Materials* (Eds.: J. Shinar, Z. V. Vardeny, Z. H. Kafafi), Marcel Dekker, New York, **2000**.

[5] a) M. Prato, M. Maggini, *Acc. Chem. Res.* **1998**, *31*, 519; b) K. E. Geckeler, S. Samal, *Polym. Int.* **1999**, *48*, 743; c) F. Diederich, M. Gomez-Lopez, *Chem. Soc. Rev.* **1999**, *28*, 263; d) A. Bianco, T. D. Ros, M. Prato, C. Toniolo, *J. Pept. Sci.* **2001**, *7*, 208; e) J.-F. Nierengarten, *New J. Chem.* **2004**, *28*, 1177; f) L. Sanchez, N. Martin, D. M. Guldi, *Angew. Chem.* **2005**, *117*, 5508; *Angew. Chem. Int. Ed.* **2005**, *44*, 5374; g) F. Diederich, C. Thilgen, *Science* **1996**, *271*, 317.

[6] a) S.-Q. Zhou, C. Burger, B. Chu, M. Sawamura, N. Nagahara, M. Toganoh, U. E. Hackler, H. Isobe, E. Nakamura, *Science* **2001**, *291*, 1944; b) E. Nakamura, H. Isobe, *Acc. Chem. Res.* **2003**, *36*, 807; c) T. Michinobu, T. Nakanishi, J. P. Hill, M. Funahashi, K. Ariga, *J. Am. Chem. Soc.* **2006**, *128*, 10384; d) J. Xiao, Y. Liu, Y. Li, J. Ye Y. Li, X. Xu, X. Li, H. Liu, C. Huang, S. Cui, D. Zhu, *Carbon* **2006**, *44*, 2785.

[7] H. Imahori, K. Tamaki, D. M. Guldo, C. Luo, M. Fujitsuka, O. Ito, Y. Sakata, S. Fukuzumi, *J. Am. Chem. Soc.* **2001**, *123*, 2607.

[8] M. Sawamura, K. Kawai, Y. Matsuo, K. Kanie, T. Kato, E. Nakamura, *Nature* **2002**, *419*, 702.

[9] E. Frankevich, Y. Maruyama, H. Ogata, *Chem. Phys. Lett.* **1993**, *214*, 39.

[10] F. Stepniak, P. J. Benning, D. M. Poirier, J. H. Weaver, *Phys. Rev. B* **1993**, *48*, 1899.

[11] a) T. Nakanishi, N. Miyashita, T. Michinobu, Y. Wakayama, T. Tsuruoka, K. Ariga, D. G. Kurth, *J. Am. Chem. Soc.* **2006**, *128*, 6328; b) D. M. Guldi, F. Zerbetto, V. Georgakilas, M. Prato, *Acc. Chem. Res.* **2005**, *38*, 38; c) Y.-G. Guo, C.-J. Li, L.-J. Wan, D.-M. Chem, C.-R. Wang, C.-L. Bai, *Adv. Funct. Mater.* **2003**, *13*, 626; d) N. Nakashima, T. Ishii, M. Shirakusa, T. Nakanishi, H. Murakami, T. Sagara, *Chem. Eur. J.* **2001**, *7*, 1766; e) A. M. Cassell, C. L. Asplund, J. M. Tour, *Angew. Chem.* **1999**, *111*, 2565; *Angew. Chem. Int. Ed.* **1999**, *38*, 2403; f) Y. Gao, Q. Chang, W. Jiao, H. Ye, Y. Li, Y. Wang, Y. Song, D. Zhu, *Appl. Phys. B* **2007**, *88*, 89; g) M. Shirakawa, N. Fujita, S. Shinkai, *J. Am. Chem. Soc.* **2003**, *125*, 9902.

[12] a) J. H. van Esch, B. L. Feringa, *Angew. Chem.* **2000**, *112*, 2351; *Angew. Chem. Int. Ed.* **2000**, *39*, 2263; b) R. Wang, C. Geiger, L. Chen, B. Swason. D. G. Whitten, *J. Am. Chem. Soc.* **2000**, *122*, 2399; c) J. H. Jung, Y. Ono, S. Shinkai, *Chem. Eur. J.* **2000**, *6*, 4552; d) D. J. Abdallah, R. G. Weiss, *Adv. Mater.* **2000**, *12*, 1237.

[13] a) K. Oishi, T. Ishi-i; M. Sano, S. Shinkai, *Chem. Lett.* **1999**, 1089; M. Sano, S. Shinkai, *Chem. Lett.* **1999**, 1089; b) T. Ishi-i, Y. Ono, S. Shinkai, *Chem. Lett.* **2000**, 809.

[14] a) D. K. Schwartz, *Surf. Sci. Rep.* **1997**, *27*, 241; b) *Langmuir–Blodgett Films*, (Ed.: M. C. Petty), Cambridge University Press, **1996**.

[15] a) M. Sano, A. Kamino, S. Shinkai, *J. Phys. Chem. B* **2000**, *104*, 10339; b) M. Matsumoto, K. Tanaka, R. Azumi, Y. Kondo, N. Yoshino, *Langmuir* **2004**, *20*, 8728; c) M. S. Chandra, T. P. Radhakrishnan, *Chem. Eur. J.* **2006**, *12*, 2982.

[16] T. Akutagawa, T. Ohta, T. Hasegawa, T. Nakamura, C. A. Christensen, J. Becher, *Proc. Natl. Acad. Sci. USA* **2002**, *99*, 5028.

[17] R. Tsunashima, S.-i. Noro, T. Akutagawa, T. Nakamura, T. Karasawa, H. Kawakami, K. Toma, *J. Phys. Chem. C* **2007**, *111*, 901.

[18] a) D. Kitamoto, K. Toma, M. Hato in *Handbook of Nanostructured Biomaterials and Their Applications in Nanobiotechnology, Vol. 1* (Ed.: H. S. Nalwa), American Scientific, California, **2005**, pp. 239–271; b) T. Kitahara, M. Shirakawa, S.-I. Kawano, U. Beginn, N. Fujita, S. Shinkai, *J. Am. Chem. Soc.* **2005**, *127*, 14980.

[19] a) M. Prato, M. Maggini, C. Giacometti, G. Scorrano, G. Sandona, G. Farnia, *Tetrahedron* **1996**, *52*, 5221; b) M. Prato, M. Maggini, *Acc. Chem. Res.* **1998**, *31*, 519.

[20] On slow cooling of a 0.25 M solution below 277 K, formation of a jellylike solid was observed.
[21] N. Nakashima, T. Ishii, M. Shirakusa, T. Nakanishi, H. Murakami, T. Sagara, *Chem. Eur. J.* **2001**, *7*, 1766.
[22] a) D. C. Dahn, K. Cake, L. R. Hale, *Ultramicroscopy* **1992**, *43*, 1243; b) D. J. Keller, F. S. Franke, *Surf. Sci.* **1993**, *294*, 409; c) J. Vesenka, M. Guthold, C. L. Tang, D. Keller, E. Delaine, C. Bustamante, *Ultramicroscopy* **1992**, *42*, 1243; d) K. A. Ramirez-Aguilar, K. L. Rowlen, *Langmuir* **1998**, *14*, 2562; e) J. Loosa, A. Alexeev, N. Grossiord, C. E. Koning, O. Regev, *Ultramicroscopy* **2005**, *104*, 160.
[23] a) Y. S. Obeng, A. J. Bard, *J. Am. Chem. Soc.* **1991**, *113*, 6279; b) N. C. Maliszewskyi, P. A. Heiney, D. H. Jones, R. M. Strongin, M. Cichy, A. A. B. Smith III, *Langmuir* **1993**, *9*, 1439; c) P. Wang, B. Chen, R. M. Metzger, T. D. Ros, M. Prato, *J. Mater. Chem.* **1997**, *7*, 2397; d) J. Milliken, D. Dominguez, H. Nelson, W. R. Barger, *Chem. Mater.* **1992**, *4*, 252.
[24] a) T. Steiner, *Angew. Chem.* **2002**, *114*, 50; *Angew. Chem. Int. Ed.* **2002**, *41*, 48; b) M. Suzuki, T. Sato, H. Shirai, K. Hanabusa, *New J. Chem.* **2006**, *30*, 1184; c) G. Careri, U. Buontempo, F. Galluzzi, A. C. Scott, E. Gratton, E. Shyamsunder, *Phys. Rev. B* **1984**, *30*, 4689; d) F. Camerel, L. Bonardi, G. Ulrich, L. Charbonniere, B. Donnio, C. Bourgogne, D. Guillon, P. Retailleau, R. Ziessel, *Chem. Mater.* **2006**, *18*, 5009; e) F. Camerel, B. Donnio, C. Bourgogne, M. Schmutz, D. Guillon, P. Davidson, R. Ziessel, *Chem. Eur. J.* **2006**, *12*, 4216; f) B. Escuder, S. Marti, J. F. Miravet, *Langmuir* **2005**, *21*, 6766; g) C. Tan, L. Su, P. Xue, C. Bao, X. Liu, Y. Zhao, *J. Mol. Liq.* **2006**, *124*, 32; h) M. L. Bushey, A. Hwang, P. W. Stephens, C. Nuckolls, *J. Am. Chem. Soc.* **2001**, *123*, 8157; i) K. Hanabusa, M. Matsumoto, M. Kimura, A. Kakehi, H. Shirai, *J. Colloid Interface Sci.* **2000**, *224*, 231; j) D. J. Moore, M. E. Rerek, R. Mendelsohn, *J. Phys. Chem. B* **1997**, *101*, 8933; k) P. Sivagurunathan, F. Liakath Ali Khan, K. Ramachandran, *Z. Phys. Chem. (Muenchen Ger.)* **2007**, *221*, 273.
[25] a) M. Avrami, *J. Chem. Phys.* **1939**, *7*, 1103; b) M. Avrami, *J. Chem. Phys.* **1940**, *8*, 212; c) *Crystallization of Polymers* (Ed.: L. Mandelkern), McGraw-Hill, New York, **1964**; d) *Macromolecular Physics, Vol. 2* (Ed.: W. Wunderlich), Academic Press, New York, **1976**.
[26] a) P. Terech, *J. Colloid Interface Sci.* **1985**, *107*, 244; b) X. Y. Liu, P. D. Sawant, *Appl. Phys. Lett.* **2001**, *19*, 3518; c) X. Y. Liu, P. D. Sawant, *Adv. Mater.* **2002**, *14*, 421; d) X. Huang, P. Terech, S. R. Raghavan, R. G. Weiss, *J. Am. Chem. Soc.* **2005**, *127*, 4336; e) X. Huang, S. R. Raghavan, P. Terech, R. G. Weiss, *J. Am. Chem. Soc.* **2006**, *128*, 15341.
[27] a) D. Vollhardt, U. Retter, *J. Phys. Chem.* **1991**, *95*, 3723; b) D. Vollhardt, M. Ziller, U. Retter, *Langmuir* **1993**, *9*, 3208; c) D. Vollhardt, *Adv. Colloid Interface Sci.* **1993**, *47*, 1; d) S. Rugonyi, E. C. Smith, S. B. Hall, *Langmuir* **2005**, *21*, 7303; e) E. S. Nikomarov, *Langmuir* **1990**, *6*, 410.
[28] J.-T. Xu, J. P. A. Fairclough; S.-M. Mai, A. J. Ryan, C. Chaibundit, *Macromolecules* **2002**, *35*, 6937; S.-M. Mai, A. J. Ryan, C. Chaibundit, *Macromolecules* **2002**, *35*, 6937.
[29] M. Chikamatsu, S. Nagamatsu, Y. Yoshida, K. Saito, K. Yase, *Appl. Phys. Lett.* **2005**, *87*, 203504.

Received: March 17, 2008
Published online: July 21, 2008

